AFRL-RX-WP-TP-2010-4138

HOT ROLLING OF GAMMA TITANIUM ALUMINIDE FOIL (PREPRINT)

S.L. Semiatin

Metals Branch
Metals, Ceramics & NDE Division

B.W. Shanahan

University of Dayton

F. Meisenkothen

UES, Inc.

APRIL 2010

AIR FORCE RESEARCH LABORATORY
MATERIALS AND MANUFACTURING DIRECTORATE
WRIGHT-PATTERSON AIR FORCE BASE, OH 45433-7750
AIR FORCE MATERIEL COMMAND
UNITED STATES AIR FORCE

REPORT DOCUMENTATION PAGE

Form Approved
OMB No. 0704-0188

1. REPORT DATE *(DD-MM-YY)*	2. REPORT TYPE	3. DATES COVERED *(From - To)*
April 2010	Journal Article Preprint	01 April 2010 – 01 April 2010

4. TITLE AND SUBTITLE
HOT ROLLING OF GAMMA TITANIUM ALUMINIDE FOIL (PREPRINT)

5a. CONTRACT NUMBER
In-house

5b. GRANT NUMBER

5c. PROGRAM ELEMENT NUMBER
62102F

6. AUTHOR(S)
S.L. Semiatin (AFRL/RXLMP)
B.W. Shanahan (University of Dayton)
F. Meisenkothen (UES, Inc.)

5d. PROJECT NUMBER
4347

5e. TASK NUMBER
RG

5f. WORK UNIT NUMBER
M02R2000

7. PERFORMING ORGANIZATION NAME(S) AND ADDRESS(ES)
Metals Branch (AFRL/RXLMP)
Metals, Ceramics & NDE Division
Materials and Manufacturing Directorate
Wright-Patterson Air Force Base, OH 45433-7750
Air Force Materiel Command, United States Air Force

University of Dayton
300 College Park
Dayton, OH 45409

UES, Inc.
4401 Dayton-Xenia Road
Dayton, OH 45432

8. PERFORMING ORGANIZATION REPORT NUMBER
AFRL-RX-WP-TP-2010-4138

9. SPONSORING/MONITORING AGENCY NAME(S) AND ADDRESS(ES)
Air Force Research Laboratory
Materials and Manufacturing Directorate
Wright-Patterson Air Force Base, OH 45433-7750
Air Force Materiel Command
United States Air Force

10. SPONSORING/MONITORING AGENCY ACRONYM(S)
AFRL/RXLMP

11. SPONSORING/MONITORING AGENCY REPORT NUMBER(S)
AFRL-RX-WP-TP-2010-4138

12. DISTRIBUTION/AVAILABILITY STATEMENT
Approved for public release; distribution unlimited.

13. SUPPLEMENTARY NOTES
Journal article submitted to *Acta Materialia*. PAO Case Number: 88ABW-2010-1355; Clearance Date: 19 Mar 2010. The U.S. Government is joint author of this work and has the right to use, modify, reproduce, release, perform, display, or disclose the work. Paper contains color.

14. ABSTRACT
Metal flow and microstructure evolution during the thermomechanical processing of thin-gage foil of a near-gamma titanium-aluminide alloy, Ti-45.5Al-2Cr-2Nb, with an equiaxed-gamma microstructure was investigated experimentally and theoretically. Foils of thickness of 200 - 250 μm were fabricated via hot rolling of sheet in a can of proprietary design. The variation in gage of the rolled foils was ±15 μm except in very sporadic (local) areas with variations of approximately 60 μm relative to the mean. Metallography revealed that the larger thickness variations were associated with large remnant colonies lying in a hard orientation for deformation. To rationalize these observations, a self-consistent model was used to estimate the strain partitioning between the softer (equiaxed-gamma) matrix and the remnant colonies. Furthermore, the efficacy of pre- or post- rolling heat treatment in eliminating remnant colonies was demonstrated and quantified using a static-spheroidization model. The elimination of remnant colonies via spheroidization prior to foil rolling gave rise to improved gage control.

15. SUBJECT TERMS
titanium aluminides, rolling, deformation inhomogeneities, annealing, spheroidization

16. SECURITY CLASSIFICATION OF:			17. LIMITATION OF ABSTRACT:	18. NUMBER OF PAGES	19a. NAME OF RESPONSIBLE PERSON (Monitor)
a. REPORT	b. ABSTRACT	c. THIS PAGE			Sheldon L. Semiatin
Unclassified	Unclassified	Unclassified	SAR	40	19b. TELEPHONE NUMBER *(Include Area Code)* N/A

Standard Form 298 (Rev. 8-98)
Prescribed by ANSI Std. Z39-18

HOT ROLLING OF GAMMA TITANIUM ALUMINIDE FOIL

S.L. Semiatin, B.W. Shanahan*, and F Meisenkothen**

Air Force Research Laboratory, Materials and Manufacturing Directorate,
Wright-Patterson Air Force Base, OH 45433
* University of Dayton, 300 College Park, Dayton, OH 45409
** UES, Inc., 4401 Dayton-Xenia Road, Dayton, OH 45432

Abstract

Metal flow and microstructure evolution during the thermomechanical processing of thin-gage foil of a near-gamma titanium-aluminide alloy, Ti-45.5Al-2Cr-2Nb, with an equiaxed-gamma microstructure was investigated experimentally and theoretically. Foils of thickness of 200 - 250 μm were fabricated via hot rolling of sheet in a can of proprietary design. The variation in gage of the rolled foils was ±15 μm except in very sporadic (local) areas with variations of approximately 60 μm relative to the mean. Metallography revealed that the larger thickness variations were associated with large remnant colonies lying in a hard orientation for deformation. To rationalize these observations, a self-consistent model was used to estimate the strain partitioning between the softer (equiaxed-gamma) matrix and the remnant colonies. Furthermore, the efficacy of pre- or post- rolling heat treatment in eliminating remnant colonies was demonstrated and quantified using a static-spheroidization model. The elimination of remnant colonies via spheroidization *prior to* foil rolling gave rise to improved gage control.

Keywords: Titanium aluminides; Rolling; Deformation inhomogeneities; Annealing; Spheroidization

1. Introduction

The selection and manufacture of materials for thermal-protection systems (TPS) plays an important role in the design of future high-speed aerospace vehicles. TPS materials must withstand high temperatures and resist oxidation for long periods of time. Current designs based on ceramics, such as the TPS for the Space Shuttle, provide very light weight but require thousands of hours of maintenance between flights. If sheet and foil of thin enough gage to meet weight constraints can be made of suitable high temperature alloys, the development of more durable and easily inspected metallic systems might yield substantial operational benefits. Candidate metallic TPS materials include gamma titanium aluminide alloys and platinum-group-metal (PGM) modified superalloys [1, 2].

The manufacture of thin-gage metallic sheet and foil represents a well-developed technology for many aluminum alloys and steels. In these cases, the processing sequence usually comprises hot rolling of thick (or thin) slab, hot sheet rolling, and final cold rolling with various intermediate surface conditioning stages. Cold rolling is frequently done with multi-stand, four-high mills (for sheet) or Sendzimir reversing mills (for foil), both of which impart a high degree of thickness control. Alloys which exhibit high work-hardening rates or limited cold ductility (e.g., stainless steels, nickel-base superalloys) often require intermediate anneals as well. For other, difficult-to-work materials, such as intermetallic alloys, even small degrees of cold rolling are not possible. In such instances, other wrought methods or altogether different approaches, such as those based on solidification or vapor processing, may be necessary. The latter

methods, however, typically do not enable a high degree of microstructure control or offer the feasibility of process scale-up.

Intermetallic alloys based on the equiatomic face-centered-tetragonal compound TiAl (denoted as γ) comprise a material class which has attractive high temperature properties but very limited cold workability [1]. The room-temperature workability can be improved by adding alloying elements (e.g., Cr, V) to ductilize the γ phase, reducing the aluminum content to produce a near-gamma titanium aluminide with a two-phase microstructure (of γ plus α_2, an ordered hcp phase), or alloying to introduce some ductile β phase. Such modifications are still insufficient to produce adequate cold rollability, however. Hence, warm or hot rolling appears to be required to process near-gamma titanium aluminide materials to thin gage. To utilize conventional rolling mills, in which the rolls are not heated, some form of encapsulation or canning is also needed to minimize temperature losses during transfer of the workpiece from a preheat/reheat furnace to the rolling mill and during rolling itself. Indeed, this so-called hot-pack-rolling approach has been found to be successful for making $\gamma + \alpha_2$ *sheet* of thickness of the order of 1-2 mm [3-5].

The key considerations associated with the extension of hot-rolling practices to make $\gamma + \alpha_2$ *foil* are similar to those associated with micro-forming processes in general and thus fall into four broad categories [6]: workpiece material characteristics, tooling, equipment, and process control. For example, the anisotropy of the flow and fracture of metals can be exacerbated when there is only one or several grains across the section or if there are microstructural inhomogeneities within the material. In addition, special demands are often placed on the rigidity of tooling and equipment because of the need

for net-shape processing necessitated by the fact that post-forming machining (e.g., grinding) may be difficult or cost-prohibitive.

The objective of the present work was to establish the *metallurgical* challenges associated with hot rolling of $\gamma + \alpha_2$ foil and methods to overcome such obstacles. For this purpose, sheets of the near-gamma titanium aluminide alloy, Ti-45.5Al-2Cr-2Nb, were encapsulated in special-designed cans and rolled conventionally. As-rolled and rolled-and-heat treated microstructures were analyzed to determine those factors that may lead to deformation heterogeneity and methods to thereby reduce or eliminate such heterogeneity.

2. Materials and experimental procedures

2.1. Materials

Microstructure evolution and gage control during the hot rolling of $\gamma + \alpha_2$ *foil* was investigated using *sheet* of Ti-45.5Al-2Cr-2Nb processed per previous work [5]. The measured alloy composition (in atomic percent) was 45.1 aluminum, 1.90 chromium, 1.90 niobium, and balance titanium. The material had been initially triple arc-melted, hot isostatic pressed (to seal casting porosity), sectioned into mults, and isothermally pancake forged to a thickness of approximately 12.5 mm *via* a 6:1 reduction at 1175°C. The wrought microstructure thus produced comprised approximately two-thirds recrystallized, equiaxed $\gamma + \alpha_2$ regions and one-third remnant colonies of $\gamma + \alpha_2$ lamellae. With respect to phase equilibria, the ordered α_2 phase becomes *disordered* α above ~1125°C [7]. The alpha transus of the program material (the temperature at which $\gamma + \alpha \rightarrow \alpha$) was estimated to be 1300°C *via* heat treatment and polarized-light (optical) microscopy.

In a manner similar to that in previous work [5], square preforms were cut from the forged pancake and hot rolled to sheet (in cans of a special design) using a furnace temperature of 1260°C. After decanning and finish grinding, the thickness of the sheets so produced was between 0.8 and 1 mm.

The microstructure of the sheet product consisted of approximately 98 pct. equiaxed γ (in a matrix of transformed γ + α_2) and ≤2 pct. remnant $\gamma + \alpha_2$ lamellar colonies (Figure 1). (In backscattered-electron (BSE) images, such as those in Figure 1, the γ phase is darker, and α_2 is lighter.) Sections taken along the rolling-direction/normal-direction (RD-ND) plane and the transverse-direction/normal-direction (TD-ND) plane revealed that the remnant colonies were approximately ellipsoidal in shape. Moreover, the γ/α_2 interfaces in the remnant colonies lay close to the rolling plane (Figures 1c, d). Following the preheat sequence used for rolling (described in the next section), the remnant lamellae within each colony had a length of ~10-50 μm and thickness of ~ 0.75-1.5 μm (Figures 1e, f).

2.2. Experimental procedures

Sheets of Ti-45.5Al-2Cr-2Nb were encapsulated in special cans (designed to impart uniform deformation and enable ready extraction of the finished foil) and rolled conventionally to obtain samples for microstructure evaluation. Specifically, canned samples were hot-rolled on a two-high mill with 200-mm diameter x 300-mm wide rolls, Rolling comprised preheating (30 minutes) and reheating (2.5 minutes between each pass) in a furnace operated at 1260°C; this temperature is below the alpha transus of the titanium aluminide alloy (Figure 2) and was selected to provide good workability [9]. Each canned preform was rolled at a speed of 125 mm/s using a reduction per pass of

~12 pct. to a total thickness reduction of ~4:1. Following rolling, the workpiece was slow cooled in vermiculite and decanned.

Rolled foils were inspected for gage variations and microstructure. The microstructures were determined in the as-rolled condition as well as after heat treatment at 1200°C or 1250°°C for various times; these temperatures correspond to those at which the microstructure consists of approximately 65 or 30 percent γ, respectively. Heat treatment was done on small samples encapsuled in quartz tubes which were evacuated and backfilled with argon.

Metallography was performed on as-polished sections in a scanning-electron microscope using BSE imaging. Select electron-backscatter-diffraction (EBSD) measurements were made using a system manufactured by EDAX-TSL Division of Ametek (Draper, UT) to establish the crystallographic orientation of the γ and α_2 lamellae in remnant colonies.

3. Results

The primary results of this investigation consisted of visual and SEM characterization of as-rolled foils and SEM characterization of foil samples heat treated at 1200 or 1250°C following rolling.

3.1. As-rolled foil observations

In the rolled-and-decanned condition, foils of Ti-45.5Al-2Cr-2Nb had a smooth surface finish and were free of pinholes (e.g., Figure 3). The final thickness of the various foils was in the range of 200-250 μm. Furthermore, except for sporadic locations, the thickness of a given foil was fairly uniform with a maximum variation of approximately $\pm$15 μm relative to the mean.

The good thickness uniformity was confirmed by metallographic observations (Figure 4a). (In these and subsequent photographs, the white surface layers are nickel plating.) At higher magnification, the microstructure was found to comprise a mixture of equiaxed γ particles surrounding grains of transformed alpha (Figure 4b) and coarse colonies of γ lamellae which had not been spheroidized by the prior forging or rolling operations (Figure 4c). The latter microstructural feature was differentiated from the transformed alpha microstructure developed during cooling by γ lamellae which were thicker (and of non-uniform thickness), longer, and bent to some degree.

The size of the remnant colonies in the as-rolled foils was variable but generally lay in the range of 20-40 μm along the ND ("thickness") and 50-100 μm along the RD ("length") (Table 1). The average aspect ratio of the colonies (AR = thickness/length) was 0.35. This aspect ratio was only slightly less than that of remnant colonies in the sheet preforms, i.e., AR = 0.47. A reduction of 4:1, such as that imposed during plane-strain foil rolling, would have given rise to a decrease in the aspect ratio of each colony by a factor of 16 (= 4 x 4) if indeed it had deformed homogeneously relative to its surrounding matrix. The fact that the aspect ratio decreased relatively little suggested that the colonies were deformed only a small amount during the foil-rolling process.

In one specific case (that is to say, a lone observation in four different sections of as-rolled foil), an extremely large remnant colony was noted; its size was ~170 μm thick x 480 μm long. This colony was found to be associated with a noticeable non-uniformity in foil thickness (Figure 5), thus suggesting that it was relatively hard and underwent very limited deformation, a conclusion in accord with the colony aspect ratio measurements noted above. Moreover, several transverse metallographic sections

through this feature (i.e., lying in the TD-ND plane) revealed that the colony was of approximately equal length in both the transverse and longitudinal planes (Figure 5b). Hence, the shape of remnant colonies was deduced to be close to ellipsoidal as in the initial sheet.

The lamellae of the remnant colonies in as-rolled foil tended to lie close to the rolling plane (Figures 4c, 5c), except near the boundaries between a colony and its surrounding matrix (e.g., Figures 5a, b, d). EBSD measurements of the *crystallographic* orientation of the lamellae of remnant colonies in both sheet and foil (Figure 6) suggested that a <111> plane in γ and the (0001) plane in α_2 lay close to the rolling plane. (Because of the very small tetragonality of the γ phase, differentiation of the <111> planes is not possible using EBSD.) Such planes are indeed parallel to the habit plane of the lamellar γ + α_2 microstructure [10, 11]. Furthermore, the retention of the Burgers relation, i.e., $(111)_\gamma \,||\, (0001)_{\alpha_2}$ and $[110]_\gamma \,||\, [11\bar{2}0]_{\alpha_2}$, suggests that both constituents of the remnant colonies underwent very limited if any deformation during both sheet rolling and foil rolling.

The length and thickness of the γ lamellae in the remnant colonies of as-rolled foils showed a wide variation. The length of the majority of the γ lamellae was in the range ~2-20 μm; the average was ~7 μm. Their thickness varied from ~1 – 1.35 μm; the average was ~1.1 μm.

3.2. Rolled-and-heat-treated foil observations

The microstructures of rolled-and-heat-treated Ti-45.5Al-2Cr-2Nb foils consisted primarily of equiaxed γ particles and equiaxed α_2 grains (Figure 7, 8). Because the volume fractions of γ and α vary with temperature, the minor phase and the majority

phase were different at the two heat treatment temperatures. The γ phase was the majority constituent at 1200°C, and α was the major phase at 1250°C. However, at both temperatures, α grains (with α/α boundaries) appeared to be pinned by discrete γ particles. Furthermore, the average size (diameter) of the phases varied with temperature. The size of the equiaxed γ was 5.4 and 4.2 μm at 1200 and 1250°C, respectively. The corresponding sizes of the equiaxed α_2 grains were 4.7 and 7.0 μm.

There was also some evidence of remnant lamellar colonies after heat treatment, but such observations decreased with increasing heat treatment temperature and time. For heat treatments at 1200°C, there was no evidence of remnant colonies after ~3 h (Figure 7). At 1250°C, the observations were less clear (Figure 8). Based on a criterion that γ lamellae had to span at least two alpha grains to be considered to be remnant, the residual colonies were eliminated after approximately 30 minutes at 1250°C.

4. Discussion

Discussion of the results of this work focus on (1) the deformation of remnant lamellae and their effect on gage control during foil rolling and (2) the modeling of microstructure evolution.

4.1. Deformation of remnant lamellae

4.1.1. Self-consistent model of plastic flow

The observed limited deformation of remnant lamellae within a matrix of equiaxed gamma was interpreted in the context of a self-consistent model of the plastic flow of two-phase materials [12]. The plastic flow of each phase is assumed to be described by a constitutive equation of the form $\sigma_i = k_i \dot{\varepsilon}_i^m$; $\sigma(\dot{\varepsilon})$, k_i, and m denote the flow stress as a function of strain rate, the strength coefficient for the specific phase i,

and the strain-rate sensitivity (assumed to the same for both phases), respectively. The model was based on the approach developed by Hill [13] for linearly elastic solids, which was later extended to the case of rate-sensitive, incompressible materials by Suquet [14]. Subsequently, it was applied to conventional titanium alloys by Briottet, *et al.* [15] and Semiatin, *et al.* [12].

The self-consistent analysis leads to the determination of an effective strength coefficient k for the two-phase aggregate (whose overall constitutive response is assumed to be $\sigma = k\dot{\varepsilon}^m$) and the (different) strain rates in each of the two phases, namely, $\dot{\varepsilon}_1$ (for the harder phase) and $\dot{\varepsilon}_2$ (for the softer phase). The strength coefficient k and the two strain rates depend on the ratio of the strength coefficients of the individual phases, k_1/k_2, and the volume fraction of the harder phase f. The dependence of $\dot{\varepsilon}_1$ (relative to the overall imposed/aggregate strain rate, $\dot{\varepsilon}_{OV}$) on k_1/k_2 and f for m = 0.23 is shown in Figure 9a. (The behavior for m = 0.15 and m = 0.30 is similar.) Figure 9a shows that the strain rate in the harder phase is very small (relative to the overall strain rate) for large values of k_1/k_2 and small f. In essence, the soft matrix largely flows around the small volume fraction of hard phase in such cases.

4.1.2. Plastic-flow data for the self-consistent model

For the present work, the harder and softer constituents comprise the remnant colonies and the equiaxed-γ matrix phase, respectively. To apply the results in Figure 9a, pertinent values of f, k_1/k_2, and m are needed. The value of f can be estimated from the metallographic results described in Sections 2 and 3. The value of k_1/k_2 is equal to the ratio of the flow stress of the discrete constituents when subjected to the same strain rate. Literature data for the constitutive behavior of gamma titanium aluminide

alloys at hot-working temperatures are limited, however, and thus only approximate estimates k_1/k_2 and m can be obtained.

The constitutive behavior was estimated from References 5, 16-21. Specifically, the plastic flow behavior from isothermal hot compression tests on Ti-45.5Al-2Cr-2Nb with an *equiaxed* $\gamma+\alpha$ (or $\gamma+\alpha_2$) microstructure was reported in Reference 5 and is summarized in Figure 9b. This material showed a sharp dependence of flow stress on temperature and strain rate. During hot rolling of sheet and foil, the temperature drops as a result of radiation and conduction heat losses during workpiece transfer to the rolling mill and rolling itself [22]. For can designs of the sort used in the present work, such temperature drops are of the order of 20-100°C. For the strain rate imposed during rolling (~1 s^{-1}) and temperatures of the order of 1150-1200°C, the m value from the data in Figure 9b is approximately 0.25.

Information on the elevated-temperature plastic-flow behavior of $\gamma + \alpha_2$ alloys with a colony microstructure is very sparse. The results of Seetharaman and Semiatin [16] appear to be the only extensive set of data. However, this previous effort dealt with *polycolony* behavior and therefore cannot be used to deduce the orientation dependence of the flow stress of single colonies such as that which has been observed at room temperature [17-19]. On the other hand, Seetharaman and Fagin [20] performed several single-colony isothermal hot compression tests on Ti-45.5Al-2Cr-2Nb samples (with a lamellar thickness of 5 μm) at 1095°C and a strain rate of 0.1 s^{-1}. The colonies were oriented such that the lamellar interface was *parallel* to the compression direction; i.e., ϕ = 0° using the terminology of Yamaguchi and his coworkers [17, 18]. The measured flow stress in this instance was ~480 MPa, or considerably greater than

the corresponding flow stress for the equiaxed microstructure under the same deformation conditions (Figure 9b), i.e., 280 MPa. If the lamellae had been thinner, the single-colony flow stress may have been even higher due to the Hall-Petch effect. For example, the room-temperature data of Umakoshi, et al. [21] suggest that the flow stress for colonies with a lamellar thickness of 1 μm (comparable to that in present work) would be *twice* that of a material with 5 μm lamellae. For higher temperatures, the Hall-Petch contribution may be less, but has been found to still be quite noticeable, such as in conventional alpha/beta titanium alloys with a lamellar microstructure [23]. For example, the flow stress is increased by approximately one-third when the lamellar thickness is decreased by a factor of 5 for this material. Hence, the ratio of the flow stress of a colony with ϕ = 0° to that of material with an equiaxed microstructure at 1095°C, 0.1 s^{-1} is of the order of 2.3 (=1.33x480/280).

The lamellar interface of the remnant colonies in the sheet and foil samples in the present work were oriented *perpendicular* to the compression direction (ϕ = 90°), *not* at ϕ = 0°. In these instances, the colony flow stress can be much higher. At room temperature, for example, the ratio of the flow stress of colonies oriented at ϕ = 90° and ϕ = 0° is ~1.8 [17, 18]. Assuming a similar dependence at the hot-working temperatures pertinent to the present work, the ratio of the flow stresses of the remnant colonies and equiaxed grains (and thus the value of k_1/k_2) is taken to be 4 ($\approx$ 2.3 x 1.8).

A similar value of k_1/k_2 is obtained if attention is focused only on the α phase of the remnant colonies. These lamellae have their c-axis close to the normal direction of the sheet/foil, and thus would require <c+a> slip to deform homogeneously. The <c+a> slip systems in the disordered α phase have a critical resolved shear stress ~3 - 3.5

times that for basal <a> or prism <a> slip [24], or the modes probably activated in the arbitrarily oriented matrix α-phase grains. Combined with the ~33 pct. increment due to the Hall-Petch effect [23], a fourfold higher flow stress for the remnant lamellae seems reasonable from this perspective as well.

4.1.3. Application of self-consistent model

The self-consistent model was applied to interpret the observed the retention of the remnant colonies during the rolling of Ti-45.5Al-2Cr-2Nb sheet into foil. Except for the sporadic very large colony noted in Section 3.1, the remnants comprised approximately 2 pct. or less of the microstructure. Thus, $f \approx 0.02$. For this value of f and $k_1/k_2 = 4$, the strain accommodated by the colonies would be only ~2 pct. of the imposed strain per Figure 9a. This prediction is in line, at least qualitatively, with the observed small change in the aspect ratio of the colonies compared to that expected if the colonies and equiaxed matrix phase had deformed under isostrain conditions. Furthermore, it can be concluded that the small flow pattern irregularities introduced by these remnant colonies would have had little effect on overall thickness uniformity associated with the specific can design.

The situation for the large rogue colony (Figure 5) is somewhat different. Its height suggests that it comprised a sizeable fraction of the original thickness of the sheet *before* foil rolling; i.e., 0.162 mm/0.8 mm = 0.2. For f = 0.2 and $k_1/k_2 = 4$, the colony would have undergone only 10 pct. of the imposed reduction. However, as the reduction increased, the effective f of this colony would have increased as the matrix flowed around it. The micrograph in Figure 5a suggests that f increased to ~0.5 by the end of the rolling operation. For f = 0.5, the colony would have deformed at a rate of

~0.35 times the imposed strain rate. Because the final aspect ratio of this colony (Table 1, last entry for foil) is comparable to that of the other (smaller) remnant colonies, however, it is unlikely that it deformed much during the entire foil rolling process. In fact, the lower overall reduction at the location of this colony (Figure 5a) suggests that the deformation process here was in fact three-dimensional in nature with larger strains on either side of the colony. Therefore, the assumption of plane sections remaining plane implicit in the application of the self-consistent model to the steady-state rolling process is inappropriate here, and a 3D FEM analysis of the flow pattern would be useful.

4.2. Microstructure evolution

4.2.1. Matrix microstructure

Measurements of the α grain sizes developed during heat treatment of foil samples at 1200 and 1250°C were interpreted in the context of the classical pinning models of Zener and Smith [25], Hellman and Hillert [26], and Hazzledine and Oldershaw [27]. These models, typically valid only for volume fractions of particles less than 0.01 [25] or less than 0.1 [26, 27], lead to the following relations:

Zener and Smith: $D_L = (4/3)\, r_p/f_p$ (1)

Hellman and Hillert: $D_L = 2r_p(6/f_p)^{1/3}$ (2)

Hazzledine and Oldershaw: $D_L = 5.6r_p(1/f_p)^{1/3}$ (3)

In Equations (1) – (3), D_L denotes the pinned grain *diameter*, and r_p is the *radius* of the pinning particles whose volume fraction is f_p.

In the present work, α grains were pinned by γ particles. All of the α grain sizes predicted using Equations (1) - (3) were *larger* than the measurements, typically by a

factor of 2 to 3. The only exception to this trend was the Zener-Smith prediction for 1200°C, which was ~10 pct. greater than the measurement.

The observed differences between measured and predicted α grain sizes may lie with the large volume fraction of γ pinning particles (which greatly exceeded 0.1 at both temperatures) as well as limitations associated with the various models themselves. For example, Manohar, et al. [28] has collected a large number of measurements for different materials with $f_p \leq 0.1$. Much of these data suggest a linear dependence of D_L on r_p/f_p, as in the Zener-Smith relation, but with a proportionality constant of 0.17 instead of 4/3. In other work, Sargent, et al. [29] and Semiatin, et al. [30] found a linear dependence of D_L on r_p/f_p with a proportionality constant between 0.84 and 1.14 for samples of Ti-6Al-4V (w/o) with $f_p \sim 0.2$. In this former work, material with a range of grain sizes was obtained by subjecting samples to various coarsening heat treatments at 775 or 815°C. The current data for Ti-45.5Al-2Cr-2Nb follow the same trend as that for Ti-6Al-4V (Figure 10).

4.2.2. Elimination of remnant lamellar colonies

The elimination of colony remnants during heat treatment is most likely driven by a reduction in overall surface energy. Two mechanisms can be postulated for the process: (a) a coarsening-type phenomenon during which mass (i.e., solute) is transferred from the ends of lamellar γ platelets through the α matrix to the broad faces of *adjacent* platelets, eventually leading to spheroidization or (b) a spheroidization mechanism per se during which mass is transported from the ends to the broad faces of the same platelet. The driving force is the same in both cases. It is the difference in matrix composition near the platelet end (whose radius is approximately equal to one-

half of the platelet thickness) and the broad face of a platelet (of approximately infinite radius), and can be quantified using the Gibbs-Thompson equation [31]. The principal difference between the two processes lies in the diffusion distance.

There does not appear to be an analysis in the literature for the coarsening of platelets whose spatial arrangement is random; i.e., the geometry suggested by micrographs for the present material. Nevertheless, it may be hypothesized that such a platelet coarsening process might lead to γ particles whose size is quite large compared to that of the γ particles in the equiaxed $\gamma + \alpha_2$ matrix. A comparison of the size of the γ particles near and away from the perimeter of remnant colonies which have been heat treated does not show this (e.g., Figures 7a, b). By contrast, the volume of remnant lamellae measuring ~1 μm thick x 7 μm diameter on average (i.e., ~38 μm^3) is approximately equal to that of spherical particles whose diameter is equal to that of the γ observed particles (i.e., ~4.5 μm). Hence, the kinetics of elimination of remnant lamellae was analyzed in the present work in the context of a relatively straightforward spheroidization mechanism.

The time τ_{vd} to complete static spheroidization via volume diffusion was estimated using an approach originally developed by Courtney and Malzahn Kampe [32] and later extended by Semiatin, *et al.* [33] for pancake-shaped precipitates such as the γ lamellae in the present case. Denoting the thickness of the platelet as d_γ and its diameter as w, τ_{vd} is given by the following expression:

$$\frac{\tau_{vd}}{\tau'} = \frac{\xi^3 - [0.328\xi^{7/3}\left(1+\sqrt{1-0.763\xi^{-4/3}}\right)^2]}{4[\frac{2(1+\xi)}{3(0.5-0.572\xi^{-1/3})} + \frac{0.5\xi^{1/3}+0.665\xi^{2/3}}{3(0.143+0.934\xi^{-1/3})}]} \quad . \qquad (4)$$

In Equation (4), $\xi \equiv w/d_\gamma + 0.5$, and the normalization constant $\tau' \equiv d_\gamma^3 RT/D_\alpha C_F \Gamma_{\gamma\alpha} V_M$; R is the gas constant, T is the absolute temperature, D_α is the diffusivity of the rate limiting solute through the alpha matrix, $G_{\gamma\alpha}$ is the γ–α interface energy, and V_M is the molar volume of the γ precipitate. The composition factor C_F is defined as follows:

$$\text{Composition Factor, } C_F = \frac{C\alpha(1-C_\alpha)}{(C_\gamma - C_\alpha)^2[1+\partial \ln r/\partial \ln C_\alpha]} \qquad (5)$$

In this relation, C_α and C_γ are the equilibrium concentrations (in atomic fractions) of the rate-limiting solute in the α and γ phases, respectively. The bracketed term in the denominator of Equation (5) is a thermodynamic factor; r denotes the activity coefficient for the rate limiting solute in the α phase.

Input parameters for the spheroidization analysis comprise D_α, C_F, $G_{\gamma\alpha}$, and V_M. The partitioning of Cr and Nb between the γ and α phases is limited; hence D_α was taken to be the diffusivity of aluminum in the α phase. For this purpose the measurements of Kainuma and Inden [34] for high-aluminum-content α were used; viz., D_α = 0.025 $\mu m^2/s$ at 1200°C and D_α = 0.0429 $\mu m^2/s$ at 1250°C. Taking the thermodynamic factor to be equal to unity, the values of C_F for aluminum were estimated from the pseudobinary phase diagram (Figure 2); C_F (1200°C) = 72.2 and C_F (1250°C) = 104.4. Because the foil samples had undergone deformation during various forging and rolling operations, the γ–α interface energy was assumed to be typical of an incoherent interface, and $\Gamma_{\gamma\alpha}$ was taken to be identical to that used in the spheroidization analysis for hot worked alpha/beta titanium alloys [33]; i.e., $\Gamma_{\gamma\alpha}$ = 0.4 J/m^2. The molar volume of TiAl was estimated to be 9600 mm^3/mol.

Using Equations (4) and (5), the spheroidization times at 1200 and 1250°C were calculated for several different platelet thicknesses and diameters representative of the values spanning the majority of the metallographic observations (Table 2). At 1200°C, the predicted times were of the order of 1-2 hours for platelet diameters comparable to the average diameter (7 μm); for heat treatment at 1250°C, the predicted times were ~0.25 to 0.5 hours for such platelet diameters. These times are similar to those found experimentally. At both temperatures, the predicted times were approximately six times longer for platelets of twice the average diameter, thus, suggesting that some remnant platelet features may be retained to long times.

4.3. Validation trial

The efficacy of pre-rolling spheroidization to eliminate sporadic rogue colonies and local thickness inhomogeneity was demonstrated by hot rolling a preform that had been given an initial heat treatment at 1250°C for 2 h. This material showed a homogeneous equiaxed microstructure before and after rolling. The surface finish of the as-decanned material following rolling was outstanding; the average surface roughness (R_a) was ~3 μm.

5. Summary and conclusions

Samples of Ti-45.5 Al-2Cr-2Nb sheet with a microstructure of equiaxed $\gamma + \alpha_2$ and isolated remnant colonies were hot rolled to foil with a final thickness of 200-250 μm. The final gage of the foils showed small variations (≤ 5 pct.) except in one region which was found to have a very large remnant colony. It was also established that the remnant colonies could be eliminated by heat treatment at 1200-1250°C for times of the order of 0.5 – 3 h. The following conclusions were drawn from this work:

(1) As suggested by a self-consistent model of the plastic flow of two-phase microstructures, unspheroidized colonies which are retained following breakdown forging and sheet rolling tend to undergo limited deformation because they have orientations characterized by a flow stress which is much higher than that of the surrounding equiaxed matrix.

(2) Remnant colonies whose size is much less than that of the sheet/foil thickness do not affect the final thickness uniformity. On the other hand, colonies whose size is comparable to the final foil thickness can result in noticeable gage non-uniformity.

(3) The size of equiaxed α_2 grains following hot working and heat treatment is smaller than that predicted by classical pinning models, but comparable to previous observations for alpha/beta titanium alloys with a high volume fraction of second-phase particles.

(4) The time to eliminate lamellae in remnant colonies during post-rolling heat treatment can be estimated using a relatively simple spheroidization analysis.

Acknowledgements- This work was conducted as part of the in-house research activities of the Metals Processing Group of the Air Force Research Laboratory's Materials and Manufacturing Directorate. The support and encouragement of the Laboratory management and the Air Force Office of Scientific Research (Dr. Joan Fuller, program manager) are gratefully acknowledged. The assistance of T. Brown, J. Brown, T. Goff, and G. Wiseman in conducting the experimental work is much appreciated. Two of the authors were supported through Air Force Contracts FA8650-09-2-5800 (BWS) and FA8650-08-D-5200 (FM).

References

[1] Kim YW. J Metals 1989; 41(7): 24.

[2] Gleeson B, Wang W, Hayashi S, Sordelet DJ. Mater. Sci. Forum 2004; 461-464: 213.

[3] Hoffmanner AL, Bhatt DD, Semiatin SL. Unpublished research, Battelle Memorial Institute, Columbus, OH 1977-1990.

[4] Semiatin SL, El-Soudani SM, Vollmer DC, Thompson CR. US Patent 5,442,847, August 1995.

[5] Semiatin SL, Seetharaman V. Metall Mater Trans A 1995; 26A: 371.

[6] Geiger M, Kleiner M, Eckstein R, Tiesler N, Engel U. Annals of the CIRP 2001; 50(2): 445.

[7] McCullough C, Valencia JJ, Levi CG, Mehrabian R. Acta Metall 1989; 37: 1321.

[8] Semiatin SL, Seetharaman V, Jain VK. Metall Mater Trans A 1994; 25A: 2753.

[9] Semiatin SL, Vollmer DC, El-Soudani SM, Su C. Scripta Metall Mater 1990; 24: 1409.

[10] Blackburn MJ. In: Jaffee RI, Promisel NE, editors. Science, Technology, and Application of Titanium. London; Pergamon Press; 1970, p. 633.

[11] Inui H, Oh MH, Nakamura A, Yamaguchi M. Phil Mag A 1992; 66A: 539.

[12] Semiatin SL, Montheillet F, Shen G, Jonas JJ. Metall Mater Trans A 2002; 33A: 2719.

[13] Hill R. J Mech Phys Solids 1965; 13: 213.

[14] Suquet PM. J. Mech Phys Solids 1993; 41: 981.

[15] Briottet L, Jonas JJ, Montheillet F. Acta Mater 1996; 44: 1665.

[16] Seetharaman V, Semiatin SL. Metall Mater Trans A 2002; 33A: 3817.

[17] Fujiwara T, Nakamura A, Hosomi M, Nishitani SR, Shirai Y, Yamaguchi M. Phil Mag A 1990; 61A: 591.

[18] Inui H, Oh MH, Nakamura A, Yamaguchi M. Acta Metall Mater 1992; 40:3104.

[19] Parthasarathy TA, Mendiratta MG, Dimiduk DM. Acta Mater 1998; 46: 4005.

[20] Seetharaman V, Fagin PN. Unpublished research, Air Force Research Laboratory, WPAFB, OH, 1991.

[21] Umakoshi Y, Nakano T, and Yamane T. Mater Sci Eng A 1992; A152: 81.

[22] Semiatin SL, Ohls M, Kerr WR. Scripta Metall Mater 1991; 25:1851.

[23] Semiatin SL and Bieler T. Acta Mater 2001; 49: 3565.

[24] Semiatin SL, Bieler TR. Metall Mater Trans A 2001; 32A: 1787.
[25] Smith CS. Trans AIME 1948: 175:47.
[26] Hellman P, Hillert M. Scand J Metall 1975; 4:211.
[27] Hazzledine PM, Oldershaw RD. Phil Mag A 1990; 61A: 579.
[28] Manohar PA, Ferry M, Chandra T. ISIJ Inter 1998; 38: 913.
[29] Sargent GA, Zane AP, Fagin PN, Ghosh AK, Semiatin SL. Metall Mater Trans A 2008; 39A: 2949.
[30] Semiatin SL, Fagin PN, Betten JF, Zane AP, Ghosh AK, Sargent GA. Submitted to Metall Mater Trans A 2009.
[31] Martin JW, Doherty RD, Cantor B. Stability of Microstructure in Metallic Systems. Cambridge (UK); Cambridge University Press; 1997.
[32] Courtney TH, Malzahn Kampe JC. Acta Metall 1989; 37: 1747.
[33] Semiatin SL, Stefansson N, Doherty RD. Metall. Mater. Trans. A 2005; 36A: 1372.
[34] Kainuma R, Inden G. Z Metallkd 1997; 88: 429.

Table 1. Dimensions of Remnant Lamellar Colonies in As-Rolled Sheet and As-Rolled Foil of Ti-45.5Al-2Cr-2Nb

Material	Colony #	Height (μm)	Length (μm)	Aspect Ratio
As-Rolled Sheet	1	25	49	0.51
As-Rolled Sheet	2	34	52	0.64
As-Rolled Sheet	3	26	77	0.33
As-Rolled Sheet	4	71	148	0.48
As-Rolled Sheet	5	26	78	0.34
As-Rolled Sheet	6	56	135	0.41
As-Rolled Sheet	7	13	35	0.38
As-Rolled Sheet	8	14	25	0.56
As-Rolled Sheet	9	37	112	0.34
As-Rolled Sheet	10	34	89	0.38
As-Rolled Sheet	11	106	135	0.78
AVG				**0.47**
As-Rolled Foil	1	32	83	0.38
As-Rolled Foil	2	22	109	0.20
As-Rolled Foil	3	23	53	0.43
As-Rolled Foil	4	37	97	0.38
As-Rolled Foil	5	167	478	0.35
AVG				**0.35**

Table 2. Predicted Times to Spheroidize Remnant-Colony Lamellae of Various Thicknesses (d_γ) and Diameters (w)

Temp (°C)	d_γ (μm)	w (μm)	C_F	τ_{vd} (h)
1200	1	7	72.2	1.02
1200	1	14	72.2	5.94
1200	1.2	7	72.2	1.76
1200	1.2	14	72.2	10.3
1250	0.8	7	104.5	0.22
1250	0.8	14	104.5	1.29
1250	1	7	104.5	0.43
1250	1	14	104.5	2.51

Figure Captions

Fig. 1. BSE images of the microstructure of the Ti-45.5Al-2Cr-2Nb (a/o) sheet used in the present investigation: (a-d) As-rolled sheet and (e, f) sheet given a preheat treatment identical to that used for foil rolling. The images were taken from: (a-c, e, f) longitudinal sections or (d) a transverse section.

Fig. 2. Pseudobinary titanium-aluminum phase diagram for alloys containing 2 atomic percent chromium and 2 atomic percent niobium [8].

Fig. 3. Macrograph of rolled-and-decanned foil.

Fig. 4. Micrographs at various magnifications taken on RD cross-sections of as-rolled foil. The white layer on the top and bottom surfaces of the foil in (a) is nickel plating.

Fig. 5. Micrographs at various magnifications showing a large remnant colony in an as-rolled foil. The sectioning plane was (a, c) the RD-ND plane and (b, d) the TD-ND plane. The white layer on the top and bottom surfaces of the foil in (a) and (b) is nickel plating.

Fig. 6. EBSD pole figures for the γ and α_2 phases of a remnant colony in (a) sheet prior to foil rolling and (b) as-rolled foil.

Fig. 7. Microstructure developed in rolled foil samples during heat treatment at 1200°C for (a) 1 h, (b) 2h, or (b) 4 h.

Fig. 8. Microstructure developed in rolled foil samples during heat treatment at 1250°C for (a) 15 min, (b) 30 min, (c) 45 min, or (d) 2 h.

Fig. 9. Self-consistent modeling of the flow behavior of two-phase microstructures: (a) Model results for the strain rate developed in the harder phase (relative to the

overall strain rate) as a function of its volume fraction and k_1/k_2 [12] and (b) isothermal, hot compression flow stress data for Ti-45.5Al-2Cr-2Nb with an equiaxed $\gamma+\alpha$ microstructure [5].

Fig. 10. Comparison of present measurements of the dependence of α grain size (D_L) in Ti-45.5Al-2Cr-2Nb samples on r_p/f_p with previous observations for Ti-6Al-4V [29, 30].

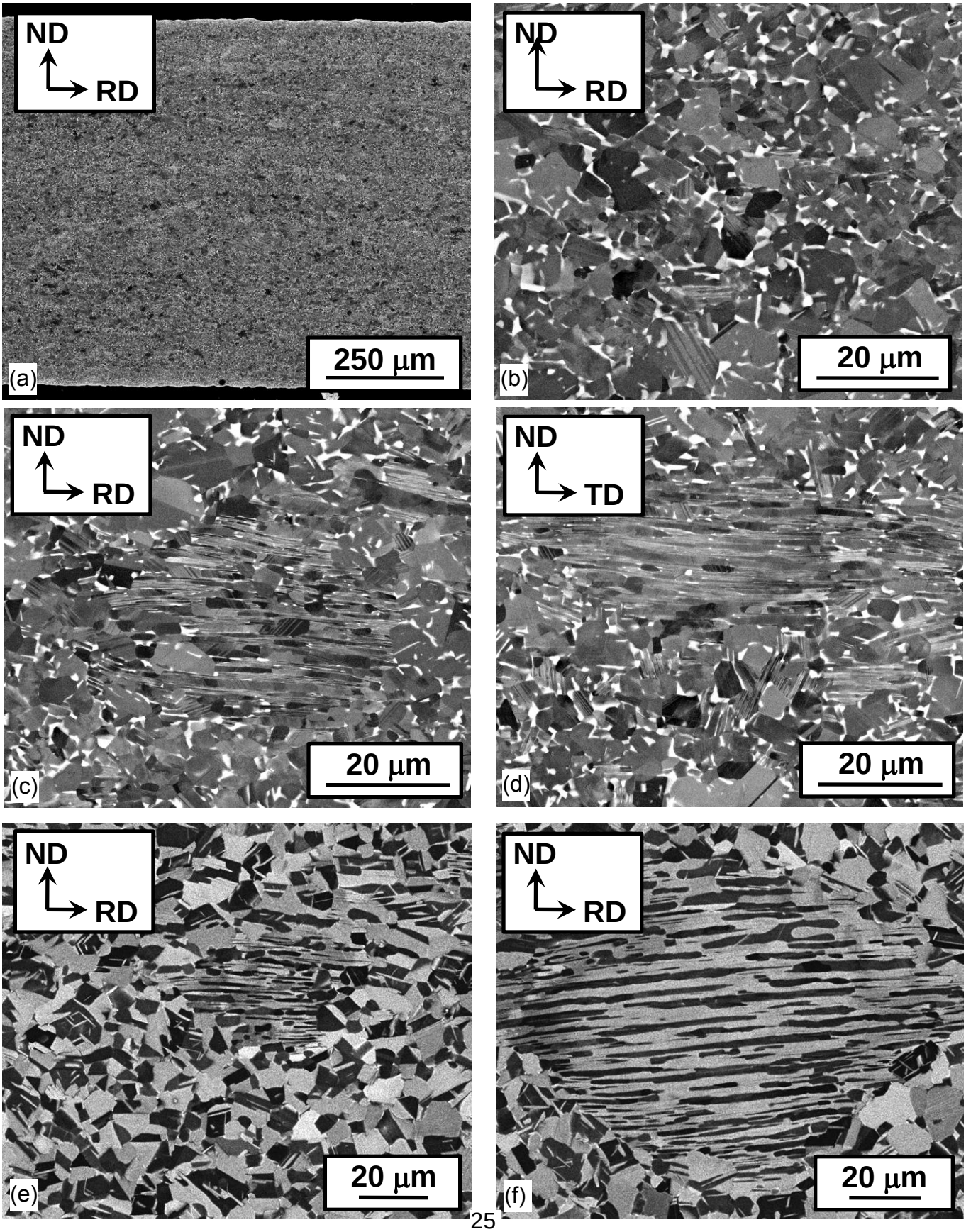

Fig. 1. BSE images of the microstructure of the Ti-45.5Al-2Cr-2Nb (a/o) sheet used in the present investigation: (a-d) As-rolled sheet and (e, f) sheet given a preheat treatment identical to that used for foil rolling. The images were taken from: (a-c, e, f) longitudinal sections or (d) a transverse section.

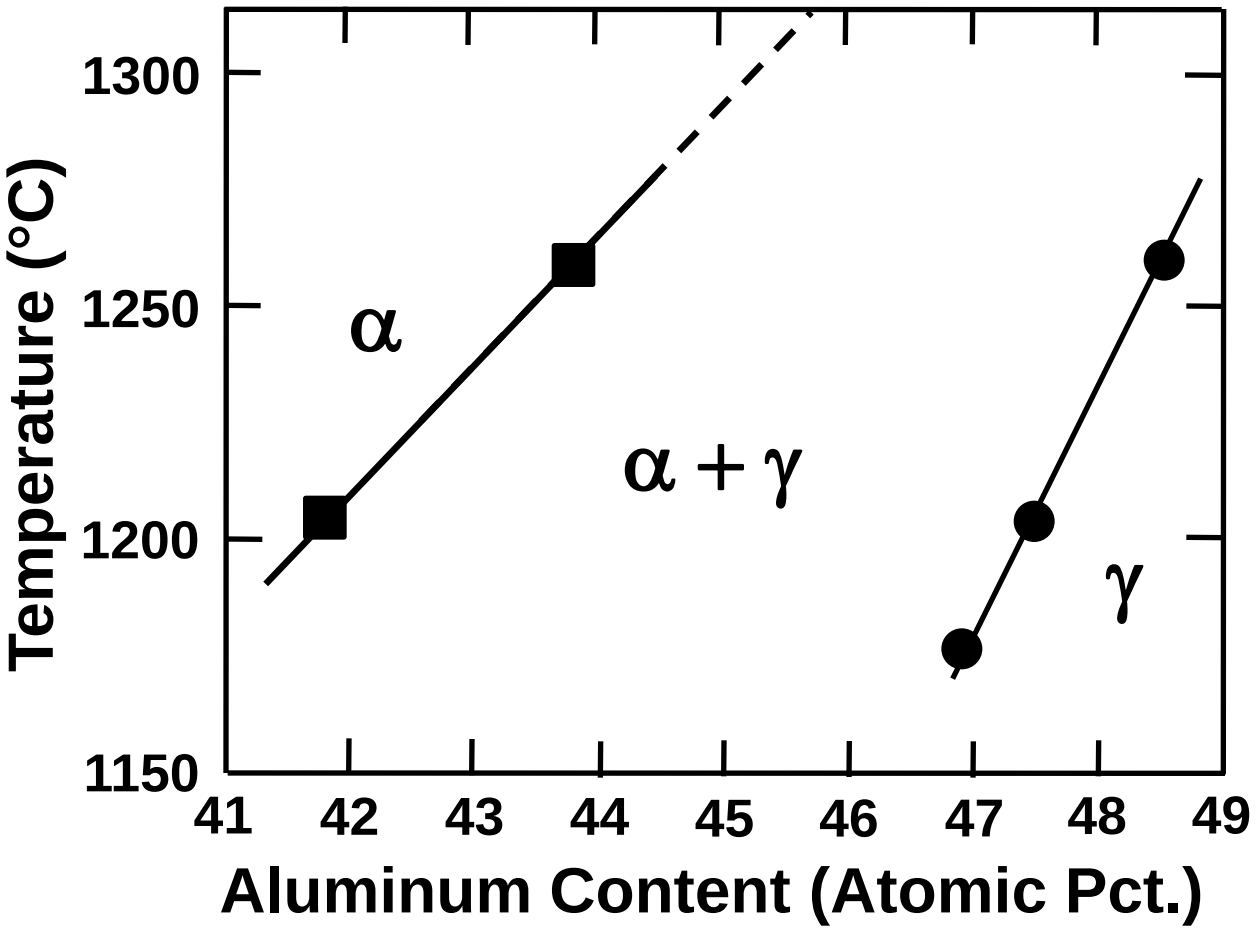

Fig. 2. Pseudobinary titanium-aluminum phase diagram for alloys containing 2 atomic percent chromium and 2 atomic percent niobium [8].

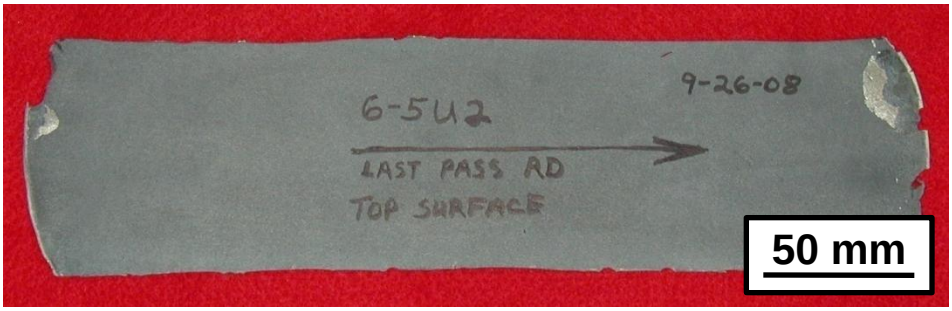

Fig. 3. Macrograph of rolled-and-decanned foil.

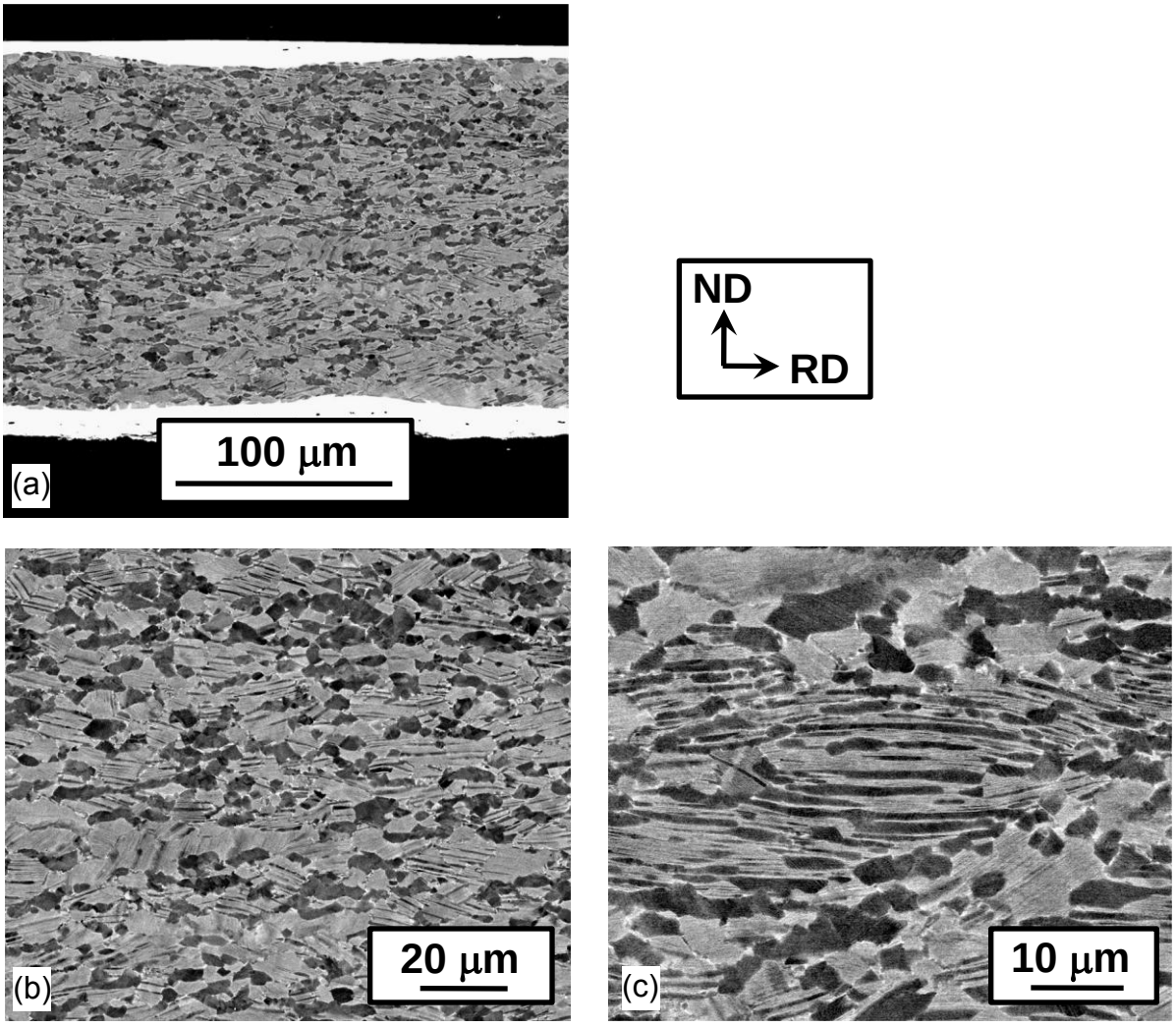

Fig. 4. Micrographs at various magnifications taken on RD cross-sections of as-rolled foil. The white layer on the top and bottom surfaces of the foil in (a) is nickel plating.

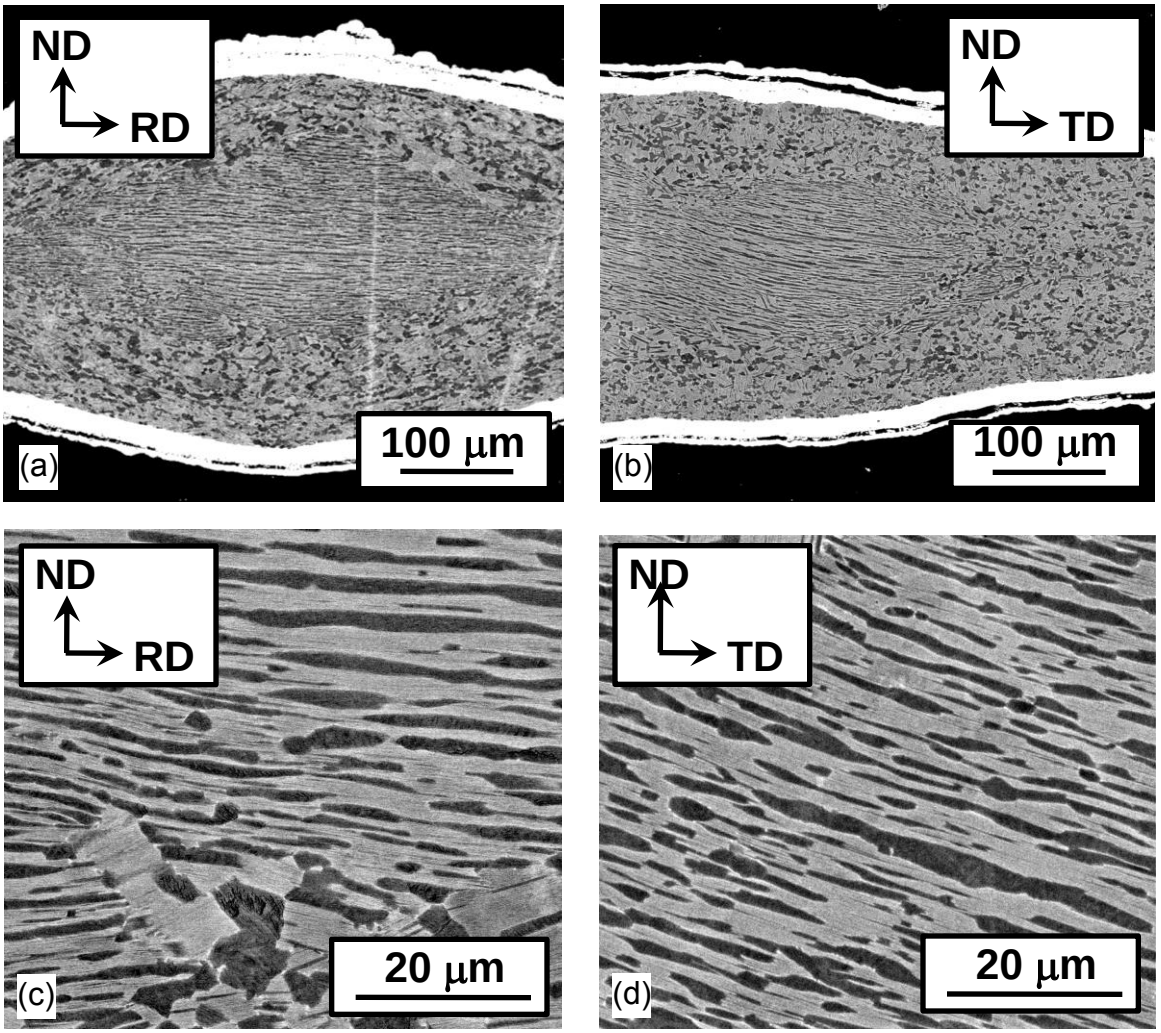

Fig. 5. Micrographs at various magnifications showing a large remnant colony in an as-rolled foil. The sectioning plane was (a, c) the RD-ND plane and (b, d) the TD-ND plane. The white layer on the top and bottom surfaces of the foil in (a) and (b) is nickel plating.

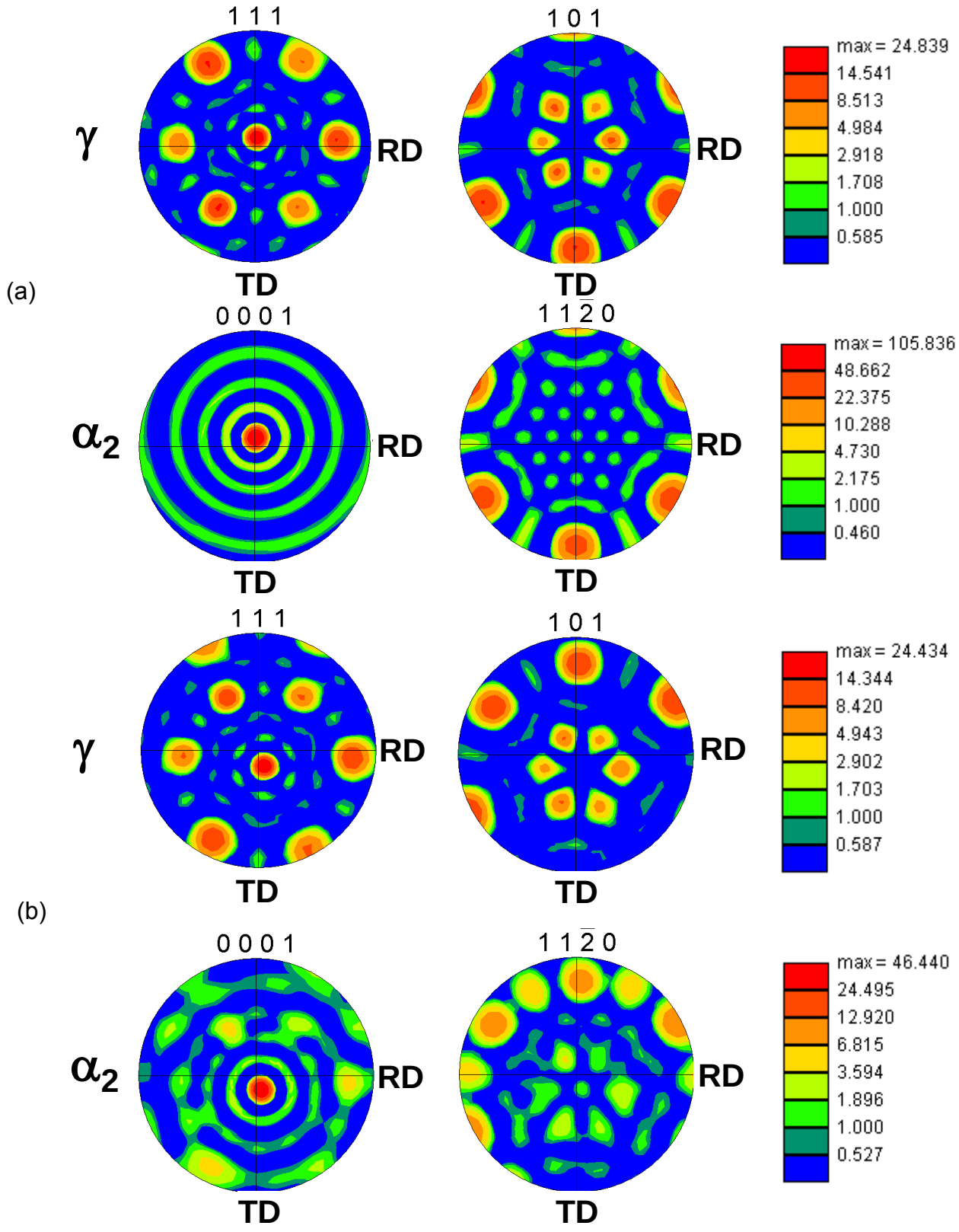

Fig. 6. EBSD pole figures for the γ and α_2 phases of a remnant colony in (a) sheet prior to foil rolling and (b) as-rolled foil.

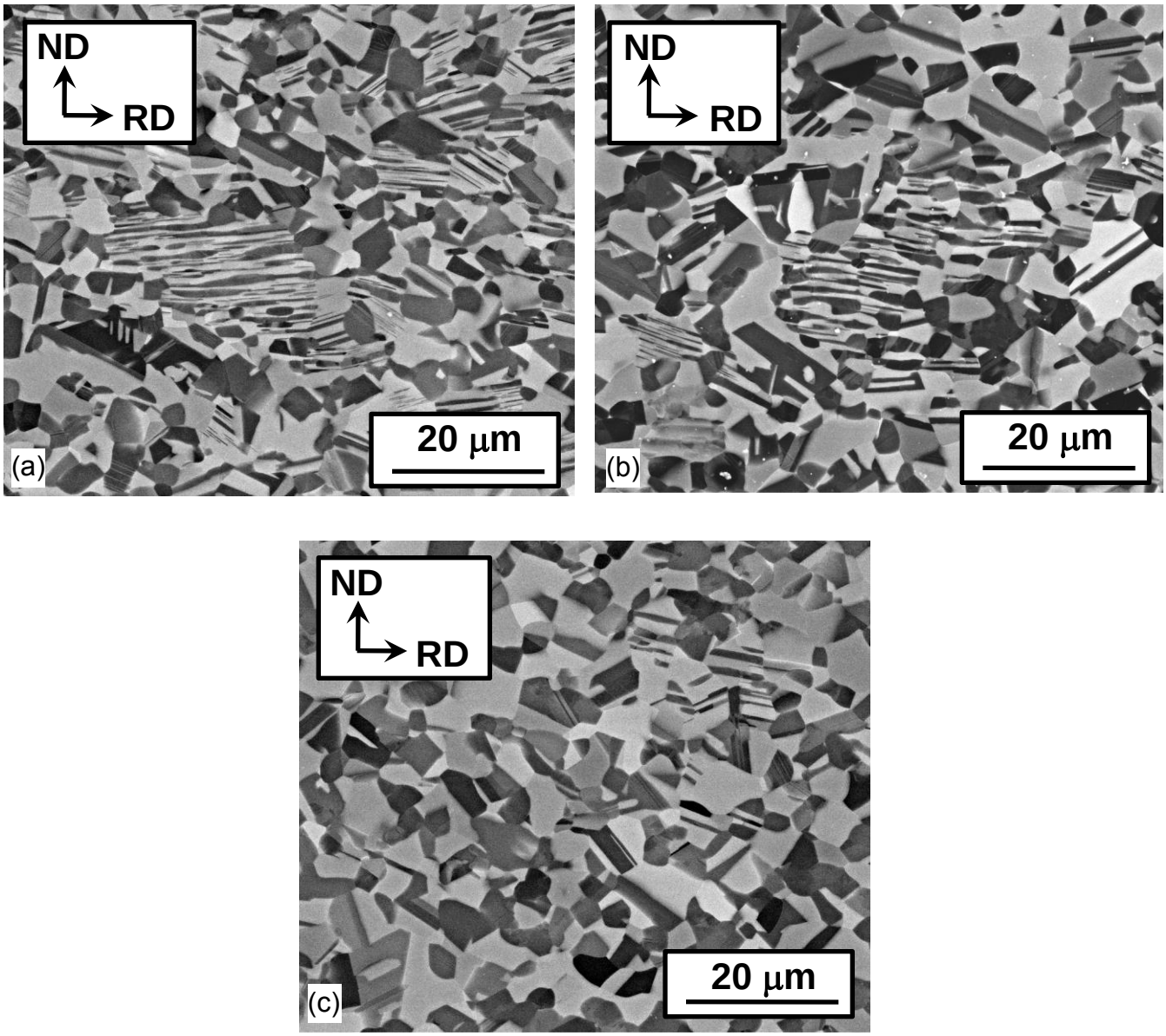

Fig. 7. Microstructure developed in rolled foil samples during heat treatment at 1200°C for (a) 1 h, (b) 2h, or (b) 4 h.

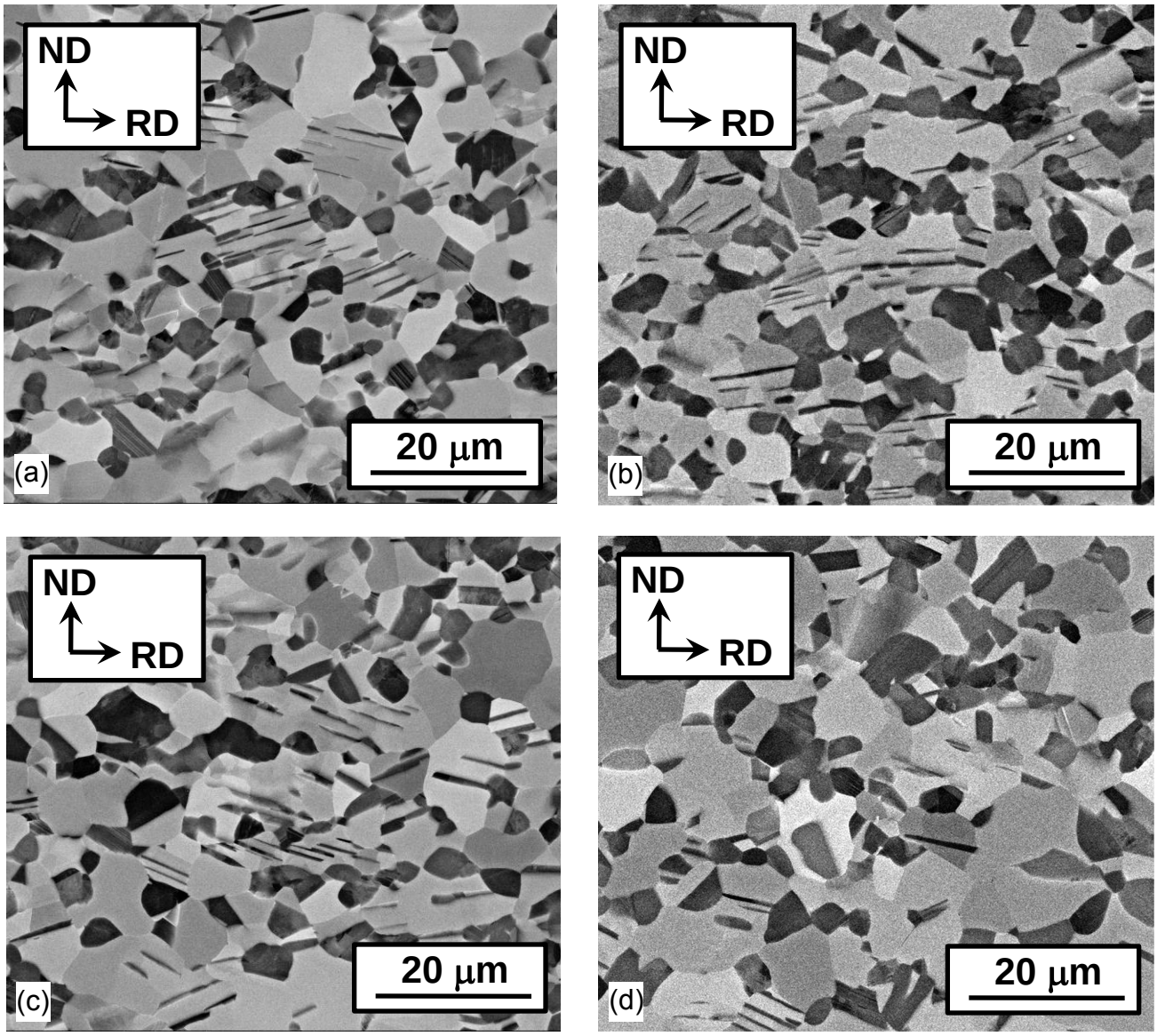

Fig. 8. Microstructure developed in rolled foil samples during heat treatment at 1250°C for (a) 15 min, (b) 30 min, (c) 45 min, or (d) 2 h.

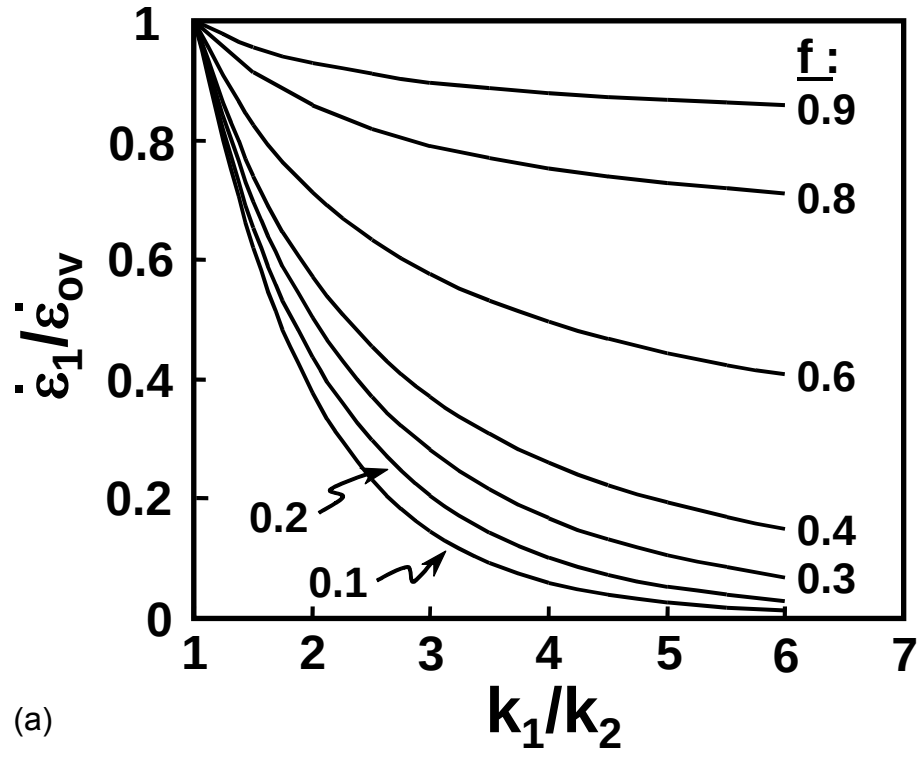

(a)

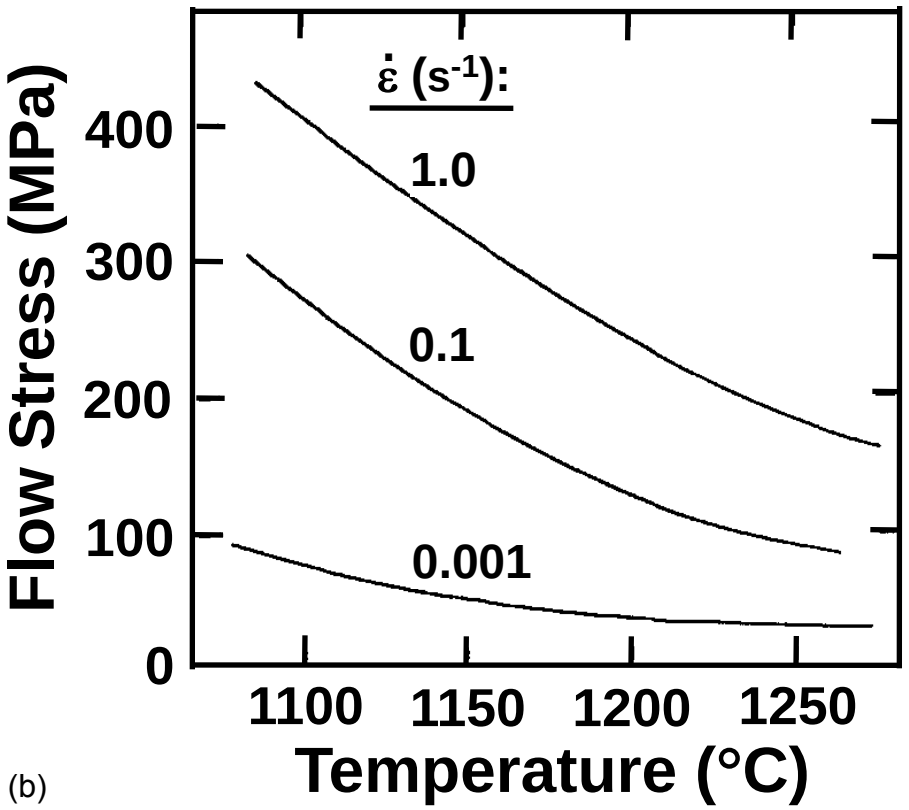

(b)

Fig. 9. Self-consistent modeling of the flow behavior of two-phase microstructures: (a) Model results for the strain rate developed in the harder phase (relative to the overall strain rate) as a function of its volume fraction and k_1/k_2 [12] and (b) isothermal, hot compression flow stress data for Ti-45.5Al-2Cr-2Nb with an equiaxed $\gamma+\alpha$ microstructure [5].

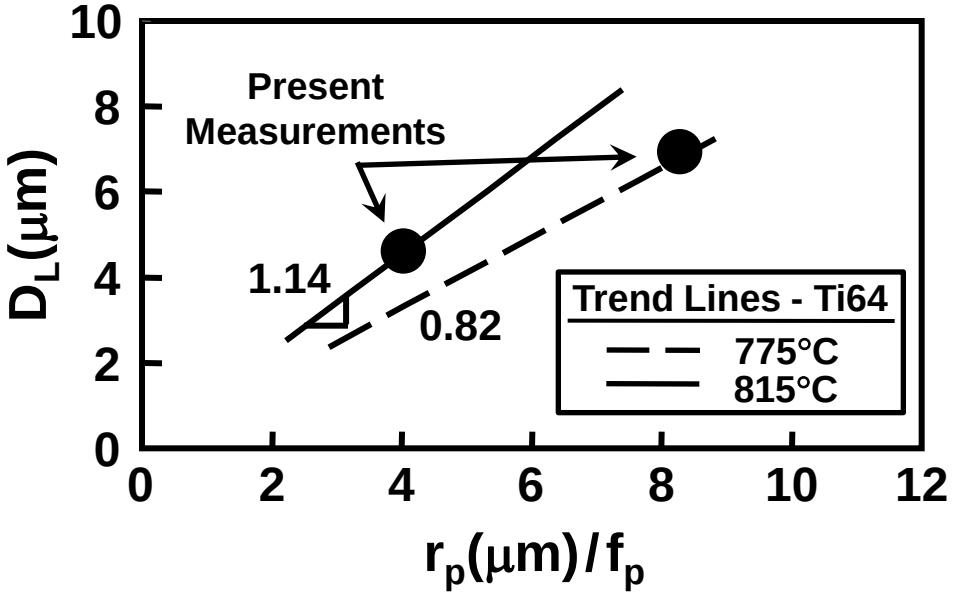

Fig. 10. Comparison of present measurements of the dependence of α grain size (D_L) in Ti-45.5Al-2Cr-2Nb samples on r_p/f_p with previous observations for Ti-6Al-4V [29, 30].